Available online at www.sciencedirect.com
ScienceDirect
Journal of Nuclear Materials 373 (2008) 269–274
journal of nuclear materials
www.elsevier.com/locate/jnucmat

Material parameters of copper and CuCrZr alloy for cyclic plasticity at elevated temperatures

J.-H. You [a,*], M. Miskiewicz [b]

[a] Max-Planck-Institut für Plasmaphysik, EURATOM Association, Boltzmannstrasse 2, 85748 Garching, Germany
[b] Department of Materials Science and Engineering, Warsaw University of Technology, Woloska 141, 02-564 Warsaw, Poland

Received 26 February 2007; accepted 8 June 2007

Abstract

In this work material parameters of cyclic plasticity for soft copper and CuCrZr alloy were determined using the combined non-linear isotropic and kinematic hardening law (the Frederick–Armstrong–Chaboche model) for the temperature range between 20 °C and 550 °C. These parameters are the initial kinematic hardening modulus, the rate of change of kinematic hardening modulus, the maximum change in the size of the yield surface and the rate of change of the yield surface size. Both precipitation-hardened and annealing-softened states were examined for CuCrZr alloy. A series of strain-controlled cyclic tension–compression tests were conducted at four temperature levels. The parameters were calibrated with the stabilised loops of stress–strain curves. The predicted stabilised loops from FEM simulation with the calibrated parameters showed good agreement with the experimental result demonstrating the validity of the considered constitutive model.
© 2007 Elsevier B.V. All rights reserved.

1. Introduction

Thanks to its excellent thermal conductivity and proper mechanical strength, copper alloys have been considered to be a candidate material for the heat sink of plasma-facing components (PFC). Especially, precipitation-hardened CuCrZr alloy was already used as heat sink material for the water cooled PFC of large scale fusion devices such as Tore Supra, JET, Wendelstein-7X and ITER (International thermonuclear experimental reactor) [1,2]. CuCrZr alloy is further considered as heat sink tube of the PFC of fusion reactors [3]. On the other hand, soft copper is often used as a stress-relieving interlayer at the bond interface between armour and heat sink in a bi-material PFC.

The cyclic high-heat-flux loads caused by the pulsed plasma operation generate a repeated thermal stress variation in the PFC structure. In this circumstance, the soft copper bond layer may preferentially suffer from alternating plastic straining (low cycle fatigue) [4,5]. Due to the strain-controlled loading nature progressive accumulation of plastic strains (incremental plastic collapse) will not occur [6]. Even the initially hardened CuCrZr heat sink may possibly experience such detrimental effect, when CuCrZr alloy undergoes irreversible softening caused by over-ageing [7]. This softening effect can occur by long term normal operation or by some accidental events.

To design a PFC with copper alloy heat sink, the possible structural failure mechanism should be identified in terms of cyclic plasticity behaviour and the structural lifetime should be assessed by computational analysis usually based on the finite element method (FEM). To this end, an appropriate material model of cyclic plasticity and corresponding materials data at elevated temperatures are needed. But, the extent of cyclic test data is normally fairly limited.

Currently cyclic stress–strain curves of hardened CuCrZr and OFHC (oxygen-free high-conductivity) copper are available for temperatures from 20 °C to 500 °C [8,9]. However, cyclic test data for over-aged (partly softened) CuCrZr are missing in the literature. Moreover, the experimentally

* Corresponding author. Tel.: +49 89 3299 1373.
E-mail address: you@ipp.mpg.de (J.-H. You).

0022-3115/$ - see front matter © 2007 Elsevier B.V. All rights reserved.
doi:10.1016/j.jnucmat.2007.06.005

identified material parameters required for FEM studies are scarcely available, since the literature data are primarily related to fatigue life measurements [10,11].

The aim of this paper is to provide the material parameters for pure copper and CuCrZr alloy in terms of the Frederick–Armstrong–Chaboche constitutive model considering the annealing effect. To this end, extensive cyclic tests were carried out for temperatures ranging from 20 °C to 550 °C. The plastic parameters were determined by the numerical regression procedure. The quality of the calibrated parameters and the effect of softening by annealing are discussed.

2. Theoretical background

The constitutive model considered in this work is based on the yield criterion of von Mises, the associated flow rule, the non-linear isotropic hardening law of Chaboche and the non-linear kinematic hardening law formulated by Armstrong and Frederick [5,12]. Being a special case of the general Chaboche hardening law, the Armstrong–Frederick hardening law takes only a dynamic recovery term into account [13,14]. The origins of the kinematic and the isotropic hardening are attributed to the Bauschinger effect and strain hardening, respectively.

Considering asymmetric hardening the von Mises yield criterion is given by

$$F = \left[\frac{3}{2}(S-\alpha'):(S-\alpha')\right]^{0.5} - \sigma_e(\varepsilon_e^{pl}) = 0, \tag{1}$$

where F denotes the plastic potential in the sense of the associated flow rule, S the deviatoric stress tensor, α' the deviatoric backstress tensor, σ_e the equivalent stress and ε_e^{pl} the equivalent plastic strain. The backstress tensor α indicates the yield surface displacement in a stress space, whereas, σ_e denotes the size of the yield surface.

The non-linear kinematic hardening law is expressed as

$$\dot{\alpha} = \frac{C}{\sigma_e}(\sigma-\alpha)\dot{\varepsilon}_e^{pl} - \gamma\alpha\dot{\varepsilon}_e^{pl}, \tag{2}$$

where $\dot{\alpha}$ denotes the backstress rate tensor, C the initial kinematic hardening modulus, $\dot{\varepsilon}_e^{pl}$ the equivalent plastic strain rate and γ a constant determining the rate at which the kinematic hardening modulus decreases with increasing plastic strains. C and γ are the material parameters to be calibrated.

The first term is the contribution of Ziegler's linear kinematic hardening and the second one is the non-linear relaxation term.

The non-linear isotropic hardening law is expressed as

$$\sigma_e = \sigma_0 + Q\cdot[1-\exp(-b\cdot\varepsilon_e^{pl})], \tag{3}$$

where σ_0 denotes the initial size of the yield surface, Q the maximum change in the size of the yield surface and b defines the rate at which the size of the yield surface changes as plastic straining progresses. Q and b are the material parameters to be calibrated.

Four material parameters of the combined hardening law can be calibrated by the fitting method using the stabilised (saturated) loops obtained from a series of strain-controlled uni-axial cyclic tension/compression tests.

Q and b are obtained from a direct fitting of the whole σ (ε^{pl}) history data to Eq. (3). C and γ can be determined using the stress–strain data on the cyclic curves of interest and the solution of Eq. (2) as suggested by the calibration procedure of the commercial FEM code ABAQUS [12].

3. Experiment

To obtain the stabilised stress–strain loops cyclic tension/compression tests were carried out with three kinds of copper metals, i.e., pure copper (99.99%), precipitation-hardened (PH) CuCrZr alloy (as-received) and annealing-softened (AS) CuCrZr alloy (heat-treated at 700 °C for 1 h). The commercial designation of the CuCrZr alloy used for the testing was Elmedur-X (CuCr1Zr, 0.8% Cr, 0.08% Zr) provided by Thyssen Duro Metall. The heat treatment temperature for the precipitation hardening was 460 °C. The AS CuCrZr alloy was included to investigate the effect of over-ageing on the cyclic hardening behaviour. The

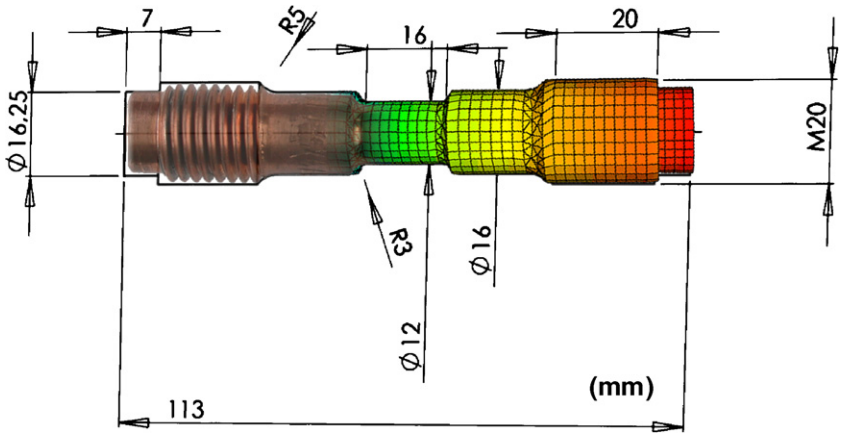

Fig. 1. Shape, dimension and finite element mesh of a copper alloy specimen used for cyclic tension–compression tests and finite element simulations.

over-aging would occur due to ripening of precipitates when a CuCrZr heat sink is exposed to long-term HHF loads. The copper specimens were also annealed for softening (heat-treated at 700 °C for 1 h).

The cyclic tests were conducted at four different temperature levels, namely, 20, 200, 400 and 550 °C. These temperatures would cover the whole temperature range which may come into question concerning the HHF operation of a heat sink. Each test was carried out up to 50 load cycles in strain-controlled mode with a fixed strain range of -0.005 to $+0.005$ and strain rate of 0.0001 s^{-1}. The half strain range 0.005 corresponds roughly to the predicted strain amplitude which would appear in a heat sink under expected HHF load.

The shape and the size of the specimens are illustrated in Fig. 1. No buckling failure was observed for this specimen geometry. The finite element mesh used for the fitting simulations is also shown.

4. Results of the cyclic tests

In Fig. 2(a) and (b), the cyclic stress–strain curves of soft copper are given for 20 °C and 400 °C, respectively. The initial stage of stress evolution is shown up to saturation. The observed cyclic hardening and thermal softening did not deviate from the literature results [15]. The cyclic stress–strain curves reach the stabilised (saturated) state within 10–15 load cycles. Such rapid saturation is ascribed to high stacking fault energy of copper which promotes the cross slip of dislocations leading to rapid stabilisation of the dislocation substructure [16]. It was observed that the saturated curve of soft copper is nearly identical to that of cold-worked copper which can be explained also by high stacking fault energy.

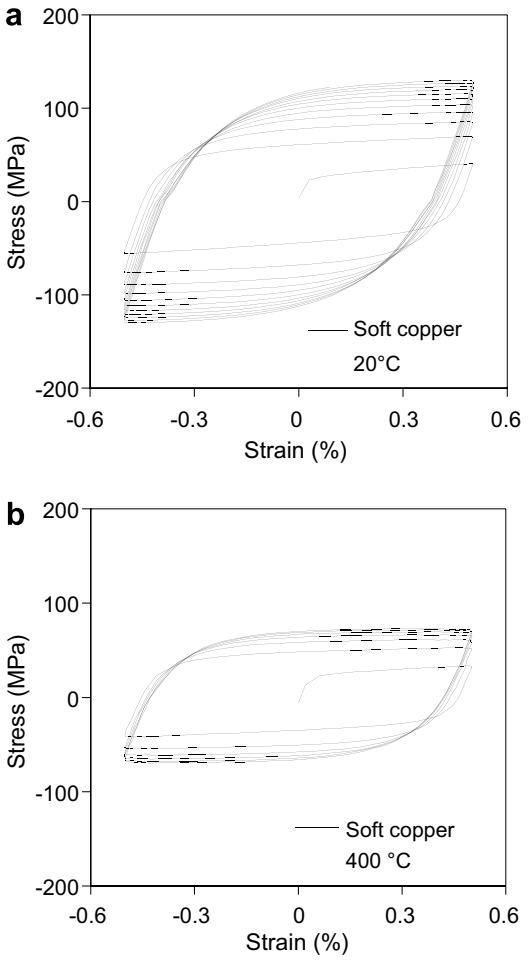

Fig. 2. Initial stage evolution of the cyclic stress–strain curve up to stabilisation measured for soft copper at (a) 20 °C and (b) 400 °C.

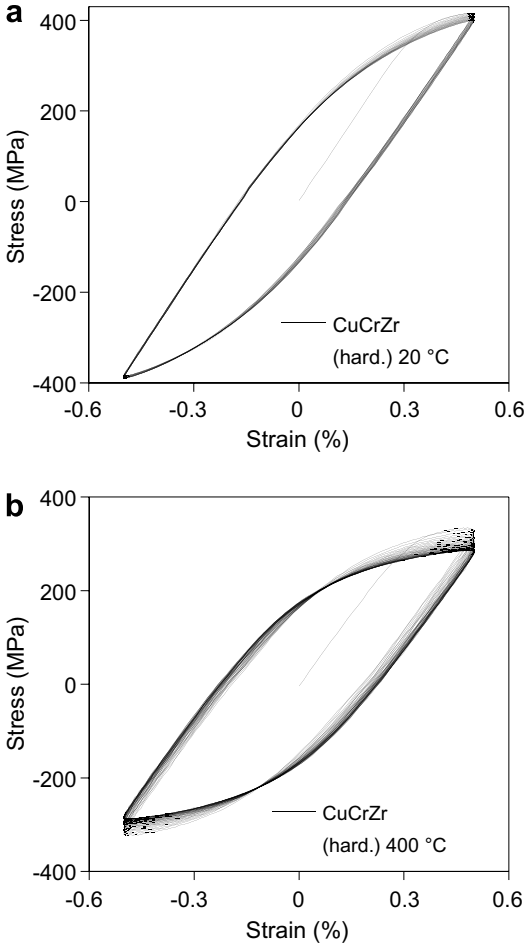

Fig. 3. Initial stage evolution of the cyclic stress–strain curve up to stabilisation measured for precipitation-hardened CuCrZr alloy at (a) 20 °C and (b) 400 °C.

Figs. 3 and 4 are the counterparts of Fig. 2 each for the case of PH CuCrZr and AS CuCrZr, respectively. The cyclic stress–strain curves of PH CuCrZr exhibit several salient features which are in contrast to the other plots. At 20 °C PH CuCrZr displayed no cyclic hardening but rather slight cyclic softening. The stress–strain response changed scarcely for the whole loading cycles so that the cyclic curves formed virtually a closed loop already from the early phase. The shape of the loop is fairly narrow indicating strong strain hardening. At higher test temperatures the characteristic cyclic softening becomes more noticeable but the shape of the loop remained unchanged.

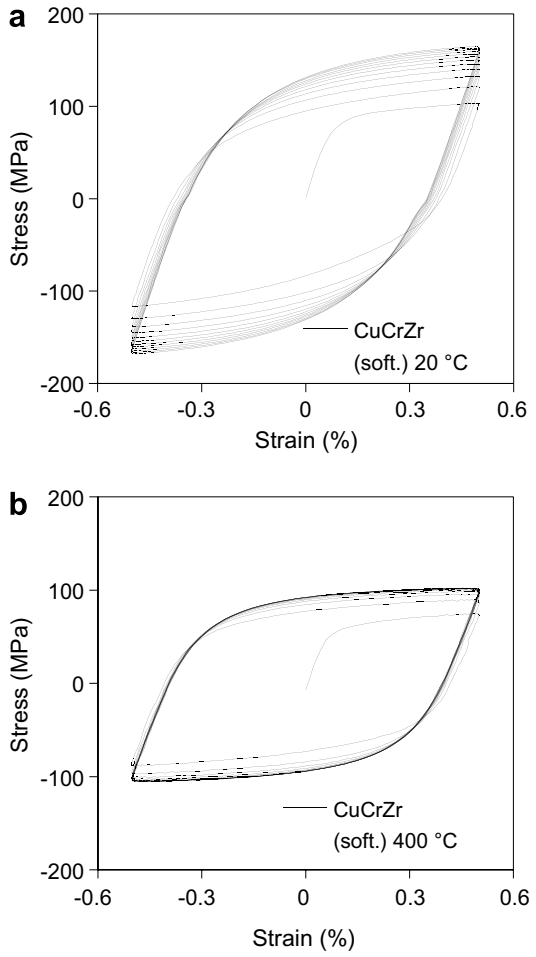

Fig. 4. Initial stage evolution of the cyclic stress–strain curve up to stabilisation measured for annealing-softened CuCrZr alloy at (a) 20 °C and (b) 400 °C.

Much more cycles were needed to achieve the saturation state.

In the case of AS CuCrZr the cyclic softening effect disappeared completely, further the normal cyclic hardening behaviour with low strain hardening rate was observed. The shape of the cyclic curves looks nearly identical to those of soft copper, although the flow stress levels of AS CuCrZr were somewhat higher than those of soft copper. This fact indicates that annealing at 700 °C for 1 h was so effective that the induced over-ageing caused significant loss of precipitation hardening. This situation will be a limit case of the microstructure change during high-heat flux operation of a PFC.

Such behaviour was already reported in the literature for a Cu–7.5% Al alloy [17]. Manson suggested a qualitative rule in regard to the propensity for cyclic strain hardening or softening as follows: initially soft metals for which the ratio of monotonic ultimate strength to 0.2% offset yield strength is larger than 1.4 exhibits cyclic strain hardening, whereas, initially hard metals for which the ratio is smaller than 1.2 shows cyclic softening [18]. According to Laird et al., the cyclic softening (i.e. Bauschinger effect) was attributed to the coarsening of a pre-existent dislocation cell substructure. The cyclic behaviour observed in this work agreed well with the general rule above.

5. Results of the plastic parameter calibration

Considering that low cycle fatigue failure occurs usually at least after several hundreds of load cycles, the parameters were calibrated using the saturation loops, since saturation in the current study was attained within 15 cycles. We utilised the built-in calibration procedure of the ABAQUS code for the Frederick–Armstrong–Chaboche model as explained in the Appendix.

The determined parameters of the three tested metals are listed for four temperatures in Tables 1–3. The negative values of Q in Table 2 are due to the cyclic softening. To calibrate the initial yield stress σ_0 further fitting process was necessary. To this end, the cyclic tension–compression tests were simulated by FEM using the already determined parameters. In ABAQUS code γ is assumed to be independent of temperature. As this is not the case here, averaged values were used.

For verification of the calibration quality the stabilised stress–strain loops of all cyclic tension–compression tests were compared with the simulated loops. For the FEM simulation exactly the same specimen geometry and boundary conditions were considered as in the actual

Table 1
Calibrated plastic parameters for soft copper

	σ_0 (MPa)	Q (MPa)	b	C (MPa)	γ
20 °C	3	76	8	64257	888
200 °C	3	60	15	44324	923
400 °C	3	36	25	31461	952
550 °C	3	16	40	17188	979
Average					935

Table 2
Calibrated plastic parameters for hardened CuCrZr

	σ_0 (MPa)	Q (MPa)	b	C (MPa)	γ
20 °C	273	−43	6	148575	930
200 °C	275	−60	8	140000	975
400 °C	238	−68	10	117500	1023
550 °C	170	−80	12	110000	1040
Average					992

Table 3
Calibrated plastic parameters for softened CuCrZr

	σ_0 (MPa)	Q (MPa)	b	C (MPa)	γ
20 °C	25	81	15	55074	729
200 °C	20	69	25	51206	858
400 °C	17	45	50	43335	1054
550 °C	18	35	75	36913	1321
Average					991

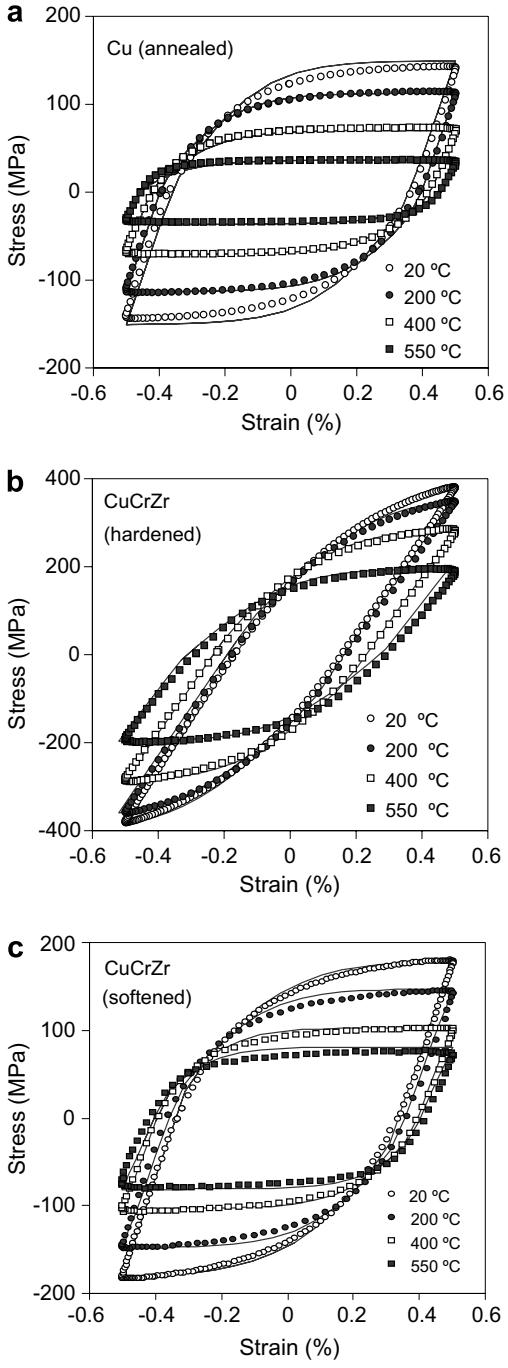

Fig. 5. Comparison of the measured stabilised stress–strain loops obtained from cyclic tension–compression tests with the numerically reproduced results from finite element simulation with the identified parameters. (a) soft copper, (b) precipitation-hardened CuCrZr and (c) annealing-softened CuCrZr. (solid lines: simulation curves, symbols: experimental data).

experiments. The results are summarised in Fig. 5(a)–(c). The FEM prediction (solid lines) coincided so well with the measured data (symbols) for all test temperatures that the solid lines are overlapped behind the symbol markers (thus nearly invisible). It should be noted that the visco-plastic effect was not included yet in the present work.

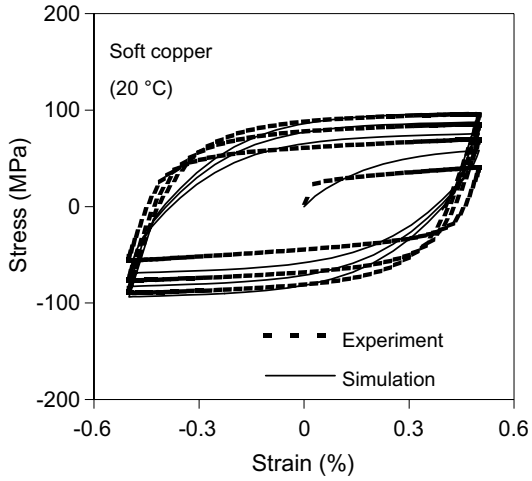

Fig. 6. Comparison of the measured initial evolution of the cyclic stress–strain curve with the model prediction by finite element simulation. The given data are for soft copper at 20 °C. (solid line: simulation curve, dotted line: experimental data).

Hence, the validity of the considered material model will be essentially restricted when creep becomes dominant.

Another related question is the validity of the parameters in the initial load cycles. For instance, the simulated initial stress–strain evolution of soft copper is compared in Fig. 6 with the experimental curve at 20 °C. It is seen that only after four cycles fairly good agreement was achieved. All other test cases showed a similar trend.

6. Summary

In this work material parameters of cyclic plasticity for soft copper and CuCrZr alloy were determined using the combined non-linear isotropic and kinematic hardening law for the temperature range between 20 °C and 550 °C. For CuCrZr both precipitation-hardened and annealing-softened states were examined.

A series of strain-controlled cyclic tension–compression tests were conducted at four temperature levels. The parameters were calibrated with the stabilised loops of stress–strain curves. The predicted stabilised loops from the FEM simulation with the obtained parameters and the considered plastic constitutive model demonstrated excellent agreement with the experimental results.

Acknowledgement

The authors are very grateful to Dr Z. Komorek, Military University of Technology, Warsaw, Poland for his kind support in performing cyclic tension/compression tests.

Appendix

For the determination of the parameters C and γ, ABAQUS requires that the original stabilised strain data ε_i^s

$(i = 1,2,\ldots,n)$ should be transformed into the modified plastic strain data $\varepsilon_i^{s,\mathrm{pl}}$. In this operation, the strain axis is at first shifted to $\varepsilon_o^{s,\mathrm{pl}}$ which is the residual plastic strain of the stabilised curve after unloading from compression and the elastic strain component is subtracted as follows:

$$\varepsilon_i^{s,\mathrm{pl}} = \varepsilon_i^s - \varepsilon_o^{s,\mathrm{pl}} - \varepsilon_i^{s,\mathrm{el}}, \tag{A.1}$$

where the superscript s denotes the data points on a stabilised stress–strain curve.

Values of α_i^s are obtained for each test data pair $\left(\sigma_i^s, \varepsilon_i^{s,\mathrm{pl}}\right)$ as

$$\alpha_i^s = \sigma_i^s - \sigma_o^s = \sigma_i^s - (\sigma_1^s + \sigma_n^s)/2, \tag{A.2}$$

where σ_o^s is the size of the stabilised yield surface under uniaxial loading.

Considering the first data pair $\left(\sigma_1^s, \varepsilon_1^{s,\mathrm{pl}}\right)$ with $\varepsilon_1^{s,\mathrm{pl}} = 0$, integration of Eq. (2) over the stabilised strain cycle gives

$$\alpha = \frac{C}{\gamma} \cdot [1 - \exp(-\gamma \cdot \varepsilon^{\mathrm{pl}})] + \alpha_1 \exp(-\gamma \cdot \varepsilon^{\mathrm{pl}}). \tag{A.3}$$

This equation is then used to calibrate the parameters C and γ.

References

[1] M. Lipa, A. Durocher, R. Tivey, Th. Huber, B. Schedler, J. Weigert, Fusion Eng. Des. 75–79 (2005) 469.
[2] ITER team, ITER-FEAT Final Design Report G A0 FDR 4 01-07-21 R 0.4, 2001.
[3] A Conceptual Study of Commercial Fusion Power Plants, Final Report of European Fusion PPCS, EFDA-RP-RE-5.0, 2004.
[4] B.I. Sandor, Fundamentals of Cyclic Stress and Strain, University of Wisconsin, Madison, 1972.
[5] J. Lemaitre, J.-L. Chaboche, Mechanics of Solid Materials, Cambridge University, Cambridge, 1990.
[6] M. Miskiewicz, J.H. You, Fusion Eng. Des., in press, doi:10.1016/j.fusengdes.2007.06.002.
[7] A.T. Peacock, V. Barabash, W. Dänner, M. Rödig, P. Lorenzetto, P. Marmy, M. Merola, B.N. Singh, S. Tähtinen, J. van der Laan, C.H. Wu, J. Nucl. Mater. 329–333 (2004) 173.
[8] ITER Structural Design Criteria for In-Vessel Components (SDC-IC) Appendix A: Materials Design Limit Data G74 MA 8 01-05-28 W 0.2, 2001.
[9] ITER Material Properties Handbook, ITER Document No. G74 MA16 (2005).
[10] A. Singhal, J.F. Stubbins, B.N. Singh, F.A. Garner, J. Nucl. Mater. 212–215 (1994) 1307.
[11] K.D. Leedy, J.F. Stubbins, B.N. Singh, F.A. Garner, J. Nucl. Mater. 233–237 (1996) 547.
[12] ABAQUS 6.6 analysis user's manual, ABAQUS Inc., Providence, 2006.
[13] J.-L. Chaboche, Int. J. Plast. 5 (1989) 247.
[14] P.J. Armstrong, C.O. Frederick, G.E.G.B. Report RD/B/N 731, 1966.
[15] J.D. Morrow, ASTM STP 378 (1965) 45.
[16] R.W. Hertzberg, Deformation and Fracture Mechanics of Engineering Materials, John Wiley & Sons, NY, 1996.
[17] C.E. Feltner, C. Laird, Acta Metall. 15 (1967) 1621.
[18] S.S. Manson, M.H. Hirschberg, Fatigue: An Introductory Approach, Syracuse University, Syracuse NY, 1964.